Laser and Particle Beams (2017), *35*, 279–285.

doi:10.1017/S0263034617000167

Tunable terahertz radiation generation by nonlinear photomixing of cosh-Gaussian laser pulses in corrugated magnetized plasma

P. VARSHNEY,[1,*] V. SAJAL,[2] A. UPADHYAY,[1] J. A. CHAKERA,[1] AND R. KUMAR[2]

[1]Laser Plasma Division, Raja Ramanna Centre of Advance Technology, Indore-452013, Madhya Pradesh, India
[2]Department of Physics and Materials Science and Engineering, Jaypee Institute of Information Technology, Noida-201307, Uttar Pradesh, India

(Received 28 September 2016; Accepted 6 February 2017)

Abstract

This paper presents a scheme of THz generation by nonlinear photomixing of two cosh-Gaussian lasers pulses having different frequencies (ω_1, ω_2) and wave numbers ($\vec{k}_1, \vec{k}_2$) and same electrical field amplitude in a corrugated plasma embedded with transverse static magnetic field. Cosh-Gaussian laser pulses have steep gradient in intensity profile along with wider cross-section, which exerts a stronger nonlinear ponderomotive force at $\omega_1 - \omega_2$ and $\vec{k}_1 - \vec{k}_2$ on plasma electrons imparting a nonlinear oscillatory velocity to plasma electrons. Oscillatory plasma electrons couple with the density ripple $n' = n_{\alpha 0}\, e^{i\alpha x}$ to produce a nonlinear current, which is responsible for resonant THz radiation at frequency $\sim \left(\omega_c^2 + \omega_p^2\right)^{1/2}$. The amplitude, efficiency and beam quality of THz radiation can be optimized by choosing proper corrugation factor (α of the plasma), applied magnetic field (ω_c), decentered parameter (b), and beam width parameter a_0 of cosh-Gaussian lasers. An efficiency of $\sim 10^{-2} - 10^{-1}$ is achieved for laser electric field $E = 3.2 \times 10^9$ V/cm.

Keywords: Cosh-Gaussian beam; Rippled magnetized plasma; Tunable terahertz generation

1. INTRODUCTION

The scientific community has wide ranging usages for the whole electromagnetic (EM) spectrum. However, the complexity of production of usable intensity differs for different parts of spectrum. The terahertz (THz) radiation is located in the spectral region 0.1–10 THz between the microwave and the infrared portion of the EM spectrum (Sizov, 2010). THz radiation has wide range of applications due to its attractive features as (Leemans *et al.*, 2004): (i) it can transmit through cloths and most packaging materials such as paper or plastics, (ii) many substances have "fingerprint" spectra in the THz range, (iii) its low photon energy (about one million times less than X rays) makes THz radiation is non-ionizing and therefore not dangerous for human beings. These properties make THz systems a promising tool for different types of applications such as medical diagnostic, quality control, biological imaging, remote sensing, material characterization, chemical & security identification, outer space communication & submillimeter radars, spectroscopic identifications of complex molecules, explosive detection (Yoshii *et al.,* 1997; Carr *et al.,* 2002; Abo-Bakr *et al.,* 2003; Dragoman & Dragoman, 2004; Leemans *et al.,* 2004; Schroeder *et al.,* 2004; Siegel, 2004), etc.

A variety of schemes have been proposed for developing THz sources, for example, interaction of short laser pulses with large band gap semiconductors (Sprangle *et al.*, 2004), metallic surfaces (Antonsen *et al.*, 2007), electro-optical crystals (Schillinger & Sauerbrey, 1999), such as ZnSe, GaP, ZnTe $LiNbO_3$. But due to lower damage threshold and low conversion efficiencies in these materials, it is not possible to generate efficient and strong THz pulses. In last few years, various plasma-based schemes have emerged as potential candidate for THz radiation generation. The plasma, being a broken medium, can handle very high fields, and can provide strong THz pulses in comparison with other mediums. Hamster *et al.* (1993) proposed a scheme of high-power THz generation from short pulse laser-produced plasma, employing 1 TW, 100 fs laser beam

*Address correspondence and reprint requests to: Prateek Varshney, Laser Plasma Division, Raja Ramanna Centre of Advance Technology, Indore-452013, Madhya Pradesh, India. E-mail: varshneyprateek28@yahoo.com

focused on gas and solid targets. They also observed THz radiation in a laser-induced plasma channel where ponderomotive force drives radiation (Hamster *et al.*, 1994). Penano *et al.* (2010) have examined a model for THz generation by the beating of the two laser beams, which generates a finite nonlinear current density due to large electron collisions driving the THz wave.

THz radiation generation by mixing of two laser beams with different intensities in different media (collisional and non-collisional plasma) has shown tremendous potential in terms of amplitude, tunability, efficiency, and directionality (Bhasin & Tripathi, 2009; Liu & Tripathi, 2009; Tripathi *et al.*, 2010; Malik *et al.,* 2011, 2012*b*; Varshney *et al.,* 2013; Singh & Malik, 2014; 2015, 2016; Varshney *et al.*, 2014; Malik, 2015). Malik *et al.* (2011) proposed a model for tunable THz radiation generation by beating of two femtosecond laser pulses. They utilized tunnel ionization mechanism for THz radiation generation with some phase difference of two laser pulses and external magnetic field. They observed significant enhancement in the frequency and power of the emitted THz radiation. Singh & Malik (2015, 2016) and Malik (2015) studied THz radiation generation by mixing of two laser beams in realistic plasma, where electron–neutral and electron–positron collisions persist. They observe lower THz field and efficiency in the collisional plasma. Few studies have also been made on tunable and efficient THz generation by using various laser profiles such as cosh-Gaussian (Singh *et al.*, 2013), Gaussian beams (Malik *et al.*, 2011, 2012*b*), super Gaussian beams (Varshney *et al.*, 2015), rounded triangular (Malik & Malik, 2013), and triangular beams (Varshney *et al.*, 2015), but most of these schemes lack on parametric studies of focusing, directionality, and collimation on generated THz wave. In particular, the cosh-Gaussian intensity profile of a laser beam that can be considered as an optical beam with null intensity at the center, has been a subject of considerable interest due to its high utility in the field of plasma, atomic, and modern optics because it can be used as an effective tool to guide, focus, and trap neutral atoms (Singh *et al.*, 2013). In the present paper, we propose a scheme of THz generation by beating of two cosh-Gaussian lasers. The cosh-Gaussian beams (decentered Gaussian beams) also have raised considerable interest in recent times on account of their wide and attractive applications. The issue of high amplitude and power of THz radiation is addressed by employing cosh-Gaussian profiles and issues of directionality and tunability are addressed by applying dc static magnetic field in the transverse direction. Both the beating lasers and generated THz radiation have the same state of polarization because the THz emission is maximum when the polarization of laser beams and the THz are aligned. The propagation properties of cosh-Gaussian laser beams are important technological issue, since these beams control higher efficient power with flat-top beam shape and hollow-Gaussian lasers beam in comparison with that of a Gaussian beam. Contrary to the case of two spatial profiles of Gaussian lasers, THz radiation can be focused at a desired position by choosing a suitable decentered parameter of cosh-Gaussian lasers. Two cosh-Gaussian laser beams exert a nonlinear ponderomotive force, which is acting on the plasma electrons. Due to velocity perturbation this ponderomotive force couples with density ripples of appropriate periodicity and excites a nonlinear current. The density ripple provides the phase-matching condition and resonant excitation of emitted radiation with an enhancement in the efficiency. In Section II, we calculate the expressions for ponderomotive force, density perturbation, and nonlinear current density. The amplitude and efficiency of THz wave are derived in Section III. Conclusion is given in Section IV.

2. BASIC EQUATIONS FOR EVALUATION OF NONLINEAR CURRENT DENSITY

We consider two cosh-Gaussian lasers with different frequencies (ω_1 and ω_2) and wave numbers ($\vec{k}_1$ and $\vec{k}_2$) co-propagating in a magnetized plasma ($B_0\,\hat{z}$) having corrugated plasma density given by $n = n_0 + n'$, $n' = n_{\alpha 0} e^{i\alpha x}$, where $n_{\alpha 0}$ is the amplitude of ripple and α is the repetition factor for corrugation ripples. These density ripples may be produced using various techniques involving transmissive ring grating and a patterned mask (Hazra *et al.,* 2004; Malik *et al.*, 2014; Malik & Malik, 2011, 2012; Kuo *et al.*, 2007). Here we can control ripple parameter by changing the groove period, groove structure, and duty cycle in such a grating and by adjusting the period and size of the masks. The profile of laser electric fields is given as

$$\vec{E}_j = \hat{y} E_0 \cosh\left(\frac{yb}{a_0}\right) e^{-y^2/a_0^2} e^{-i(\omega_j t - k_j x)}, \tag{1}$$

where $j = 1,2$ for two lasers, a_0 is the initial beam width, and b is the decentered parameter. The electric field profile given by Eq. (1) is plotted in Figure 1. One can notice that as a decentered parameter of the cosh-Gaussian laser beam changes

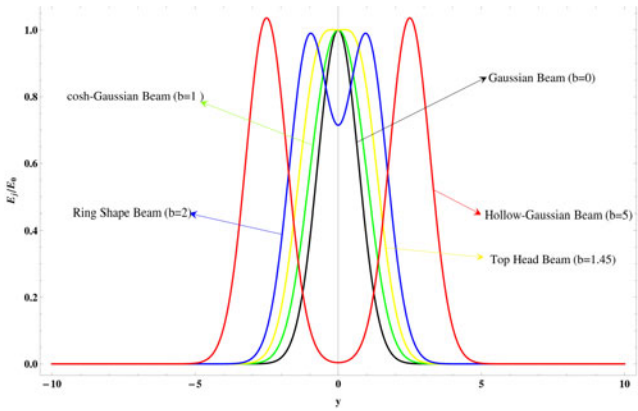

Fig. 1. Normalized cosh-Gaussian laser field amplitude as a function of transverse distance y for de-centered parameters $0 < b \leq 5$. Other laser parameters are $a_0 = 0.05$ mm, $\omega_1 = 2.4 \times 10^{14}$ rad/s.

https://doi.org/10.1017/S0263034617000167 Published online by Cambridge University Press

from $b = 0$ to 5, the profile changes its shape in the following sequences: (1) Gaussian ($b = 0$), (ii) cosh-Gaussian ($b = 1$), (iii) flat-top ($b = 1.45$), (iv) ring shape ($b = 2$), and (v) hollow-Gaussian ($b = 5$).

Beating lasers exert a nonlinear ponderomotive force $\vec{F}_p$ ($= F_{px}\hat{x} + F_{py}\hat{y}$) on plasma electron having oscillatory velocity (due to the electric field of beating lasers) $\vec{v}_j = e[-\omega_c\hat{x} + \omega_j\hat{y}]/m(\omega_j^2 - \omega_c^2)E_{jy}$ at frequency $\omega = \omega_1 - \omega_2$ and wave vector $\vec{k}'' = \vec{k}_1 - \vec{k}_2$. The components of the ponderomotive force F_{px} and F_{py} are as follows:

$$F_{px} = \frac{e^2E_0^2}{2m}[\delta_{11} - \delta_{12}\Delta]\cosh^2\left(\frac{yb}{a_0}\right)e^{-2y^2/a_0^2}, \tag{2a}$$

$$F_{py} = \frac{e^2E_0^2}{2m}[\delta_{21} - \delta_{22}\Delta]\cosh^2\left(\frac{yb}{a_0}\right)e^{-2y^2/a_0^2}, \tag{2b}$$

where $\delta_{12} = [i\omega_c\omega/(\omega_1^2 - \omega_c^2)(\omega_2^2 - \omega_c^2)]$,

$$\delta_{11} = \left[\frac{i\omega_1k_2}{\omega_2(\omega_1^2 - \omega_c^2)} - \frac{i\omega_2k_1}{\omega_1(\omega_2^2 - \omega_c^2)} - \frac{i\omega_c^2k''}{(\omega_1^2 - \omega_c^2)(\omega_2^2 - \omega_c^2)}\right],$$

$$\delta_{21} = \left[\frac{-\omega_ck_1}{\omega_1(\omega_2^2 - \omega_c^2)} - \frac{\omega_ck_2}{\omega_2(\omega_1^2 - \omega_c^2)} - \frac{\omega_c\omega_2k_2}{(\omega_2^2 - \omega_c^2)(\omega_1^2 - \omega_c^2)} - \frac{\omega_c\omega_1k_1}{(\omega_2^2 - \omega_c^2)(\omega_1^2 - \omega_c^2)}\right],$$

$$\delta_{22} = \left[\frac{2i\omega_1\omega_2}{(\omega_1^2 - \omega_c^2)(\omega_2^2 - \omega_c^2)}\right],$$

$$\Delta = -\frac{2y}{a_0^2} + \frac{b}{a_0}\tanh\left(\frac{yb}{a_0}\right),$$

where $\omega_c = eB_0/m$

Figure 2 shows the variation of ponderomotive force as a function of decentered parameter b. The ponderomotive force couples with pre-existing space-charge mode (of negligible amplitude) having potential φ at frequency $\omega = \omega_1 - \omega_2$ and wave number $\vec{k}'' = \vec{k}_1 - \vec{k}_2$, to provide oscillatory velocity to plasma electrons in the presence of transverse magnetic field, given by

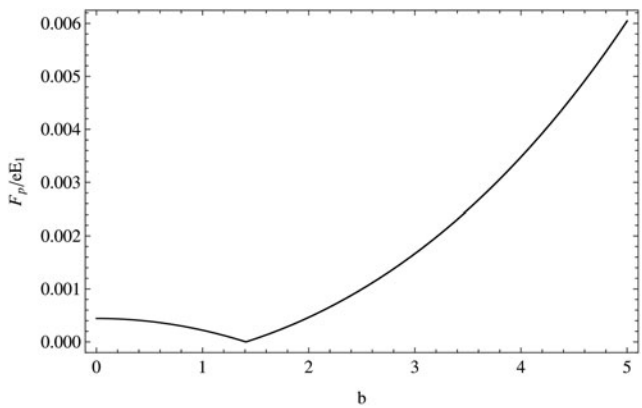

Fig. 2. Plot of normalized ponderomotive force F_p/eE_1 as a function of decentered parameter b.

$$v_x = \frac{1}{m(\omega^2 - \omega_c^2)}\left[ie\omega\nabla\varphi + \omega_cF_{py} + i\omega F_{px}\right], \tag{3a}$$

$$v_y = \frac{1}{m(\omega^2 - \omega_c^2)}\left[-e\omega_c(\nabla\varphi) - \omega_cF_{px} + i\omega F_{py}\right]. \tag{3b}$$

The oscillations of plasma electron perturb the equilibrium of plasma and, density perturbation due to this can be calculated by substituting Eq. (3) into continuity equation. The density perturbation $n = n^{NL} + n^L$ consists of both linear part (due to space-charge mode) and nonlinear part (due to the ponderomotive force). Here, density perturbation is assumed to be small as compared with the density ripple. Substituting $n = n^L + n^{NL}$ in the Poisson's equation $\nabla^2\varphi = 4\pi ne$, we obtain

$$\varphi = -\frac{4\pi e}{k^2}\frac{n^{NL}}{\varepsilon}, \tag{4}$$

where $\varepsilon = 1 + \chi$ and $\chi = -\omega_p^2/(\omega^2 - \omega_c^2)$. On rearranging Eqs. (3) and (4), we obtain the oscillatory velocity components of plasma electrons:

$$v_y = \frac{1}{m(\omega^2 - \omega_h^2)}\left[\omega_cF_{py} + i\omega F_{px}\right], \tag{5a}$$

$$v_z = \frac{-\omega_c}{m(\omega^2 - \omega_h^2)}F_{px} + i\frac{(\omega^2 - \omega_p^2)}{m(\omega^2 - \omega_h^2)\omega}F_{py}, \tag{5b}$$

where $\omega_h = \sqrt{\omega_c^2 + \omega_p^2}$. In the presence of density ripple $n_{\alpha 0}e^{i\alpha x}$, the oscillatory velocity excites a nonlinear current density at $(\omega, \vec{k}_1 - \vec{k}_2 + \vec{\alpha})$, which can be written as

$$\vec{J}^{NL} = -\frac{1}{2}n_{\alpha 0}e\vec{v}_\omega^{NL}e^{i\alpha x}. \tag{6}$$

It can be seen that the nonlinear current oscillates at frequency difference $\omega = \omega_1 - \omega_2$ similar to the ponderomotive force, but its wave number $\vec{k}(= \vec{k}_1 - \vec{k}_2 + \vec{\alpha})$ is different from the ponderomotive force.

3. THZ AMPLITUDE

Now, we solve the wave equation to find the amplitude of the THz wave

$$\nabla^2\vec{E} - \vec{\nabla}(\vec{\nabla}.\vec{E}) + \frac{\omega^2}{c^2}(\bar{\bar{\varepsilon}}\vec{E}) = -\frac{4\pi i\omega}{c^2}\vec{J}, \tag{7}$$

where $\bar{\bar{\varepsilon}}$ is the plasma permittivity tensor at ω. We can separate out the coupled $\hat{x}$ and $\hat{y}$ components of $\vec{E}$. On

https://doi.org/10.1017/S0263034617000167 Published online by Cambridge University Press

neglecting second-order term $\hat{y}$ component of THz radiation is given by

$$-\frac{2ikc^2}{\omega^2}\frac{\partial E_y}{\partial z}+\left(\frac{k^2c^2}{\omega^2}-\varepsilon_{yy}+\frac{\varepsilon_{yx}\varepsilon_{xy}}{\varepsilon_{xx}}\right)$$
$$E_y=\frac{4\pi i}{\omega}J_y^{\rm NL}-\frac{\varepsilon_{yx}}{\varepsilon_{xx}}\frac{4\pi i}{\omega}J_x^{\rm NL}, \tag{8}$$

where $\varepsilon_{yy}=[1-(\omega_p^2/\omega^2-\omega_c^2)]$ and $\varepsilon_{xy}=-i[\omega_c\omega_p^2/(\omega/\omega^2-\omega_c^2)]$ are components of the dielectric tensor. One can conclude from Eq. (8) that THz radiation generation has to satisfy the following dispersion relation for exact phase-matching condition in the corrugated magnetized plasma, which includes the corrugation factor and suggests that the maximum energy transfer from beating lasers to oscillating electrons will take place at resonance condition leading to the maximum THz radiation

$$\frac{k^2c^2}{\omega^2}=\left|\varepsilon_{yy}-\frac{\varepsilon_{xy}\varepsilon_{yx}}{\varepsilon_{xx}}\right|. \tag{9a}$$

The corrugation factor (periodicity of density ripples) required for the fine tuning of maximum energy transfer is calculated utilizing Eq. (9a) along with resonance conditions $\vec{k}=\vec{k}_1-\vec{k}_2+\alpha$ and $\omega=\omega_1-\omega_2\approx\omega_h$. The corrugation factor comes out as follows:

$$\lambda_c=\frac{2\pi}{\alpha}=\frac{2\pi c}{\omega[|(\varepsilon_{yy}-\varepsilon_{xy}\varepsilon_{yx}/\varepsilon_{xx})^{1/2}-1|]}. \tag{9b}$$

Varshney *et al.* (2013, 2015) have shown that the wave number of density ripples (α) increases with THz frequency (ω), attains maximum value at $\omega\sim\omega_h$ (resonance), and then starts decreasing. On combining Eqs. (8) and (9), we obtain the phase-matched normalized amplitude of THz radiation as follows:

$$\left|\frac{E_y}{E_0}\right|=\frac{1}{4k'}\frac{n_{q0}}{n_0}\frac{1}{\omega'(\omega'^2-\omega_h'^2)}$$
$$x'\left[\left|\left(\frac{\omega'^2-1}{\omega'}-\left|\frac{\varepsilon_{xy}}{\varepsilon_{xx}}\right|\omega_c'\right)F_{py}+\left(\omega_c'-\omega'\left|\frac{\varepsilon_{yx}}{\varepsilon_{xx}}\right|\right)F_{px}\right|\right], \tag{10}$$

where $k'=kc/\omega_p$, $\omega'=\omega/\omega_p$, $\omega_c'=\omega_c/\omega_p$, and $x'=x\omega_p/c$. Substituting the ponderomotive force into Eq. (10), we obtain normalized amplitude of THz wave as follows:

$$\left|\frac{E_y}{E_0}\right|=\left[\begin{array}{l}\xi_1'\delta_{11}'+\frac{2y'\xi_1'\delta_{12}'}{a_0'^2}-\frac{b\xi_1'\delta_{12}'}{a_0'}\tanh\left(\frac{y'b}{a_0'}\right)+\xi_2'\delta_{21}'+\frac{4y'\xi_2'\delta_{22}'}{a_0'^2}\\ -\frac{b\xi_2'\delta_{22}'}{a_0'}\tanh\left(\frac{yb}{a_0'}\right)\end{array}\right]$$
$$\cosh^2\left(\frac{y'b}{a_0'}\right)e^{-2(y'^2/a_0'^2)}, \tag{11}$$

where $y'=y\omega_p/c$, $a_0'=a_0\omega_p/c$, $\delta_{12}'=\delta_{12}/\omega_p^2$, $\delta_{11}'=\delta_{11}/c\omega_p$, $\delta_{21}'=\delta_{21}/c\omega_p$, $\delta_{22}'=\delta_{22}/\omega_p^2$,

$$\xi_1'=c\omega_p\left[\frac{1}{8k'}\frac{n_{\alpha0}}{n_0}\left(\frac{\omega'\omega_2'}{\omega'^2-\omega_h'^2}x'v_2'\left\{\omega'+\omega_c'\left|\frac{\varepsilon_{xy}}{\varepsilon_{xx}}\right|\right\}\right)\right],$$

$$\xi_2'=c\omega_p\left[\frac{1}{8k'}\frac{n_{\alpha0}}{n_0}\left(\frac{\omega'\omega_2'}{\omega'^2-\omega_h'^2}x'v_2'\left\{\omega_c'+\frac{\omega'^2-1}{\omega'}\left|\frac{\varepsilon_{yx}}{\varepsilon_{xx}}\right|\right\}\right)\right].$$

Equation (10) exhibits that greater the value of corrugation amplitude ($n_{\alpha0}/n_0$), greater will be the amplitude of excited THz radiation due to larger number of oscillating electrons involved in the process of nonlinear current generation at (ω, $\vec{k}$). In Figure 3a and 3b, the normalized THz amplitude is plotted as a function of normalized THz frequency (ω/ω_p) for different laser profiles (corresponding to decentralized parameter $b=0,\ 0.5,\ 1.0,\ 1.4,\ 3,\ 4,\ 5$) respectively at

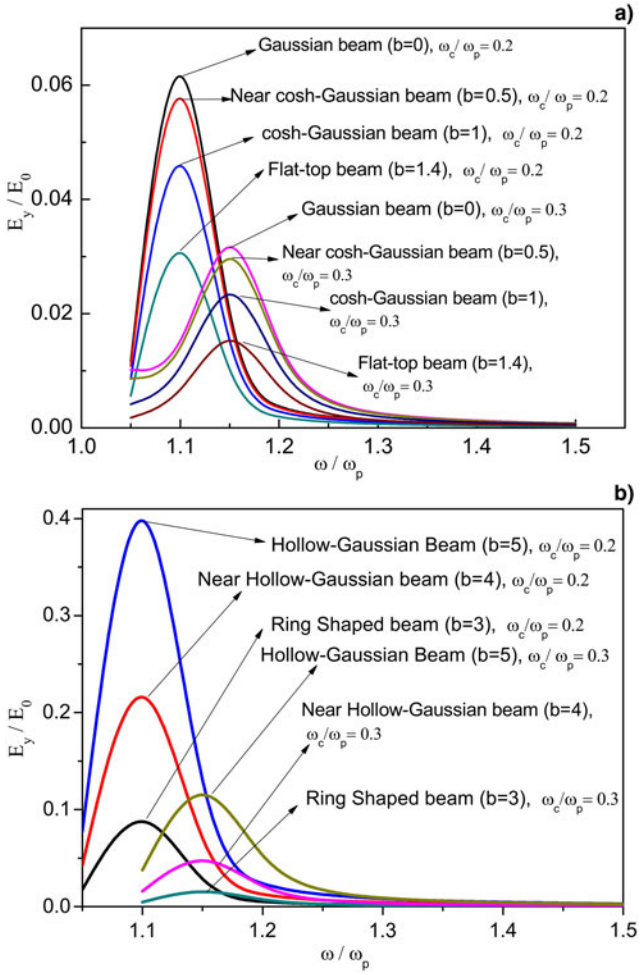

Fig. 3. (a) Plot of normalized THz amplitude (E_y/E_1) as a function of normalized THz frequency (ω/ω_p) for different values of decentered parameter $0<b\le1.4$. All other parameters are same as Figure 1. (b) Plot of normalized THz amplitude (E_y/E_1) as a function of normalized THz frequency (ω/ω_p) for different values of decentered parameter $1.5<b\le5$. All plasma parameters are same as Figure 1.

https://doi.org/10.1017/S0263034617000167 Published online by Cambridge University Press

$\omega_c/\omega_p = 0.2$ ($B_0 = 71$ kG) and $\omega_c/\omega_p = 0.3$ ($B_0 = 107$ kG). The maximum THz amplitude is obtained at resonance condition $\omega \approx \omega_h$ irrespective of laser profiles. It can be attributed to the factor $(\omega^2 - \omega_h^2)$ present in the expression of nonlinear current $\vec{J}_{NL}$ given by Eq. (6) (in $\vec{v}_\omega^{NL}$). This factor is introduced in Eq. (4) (potential φ of space charge mode of plasma) due to the presence of perpendicular magnetic field. In the presence of magnetic field, the potential of space-charge mode will achieve its peak value at $\omega \cong \omega_h$ and energy transfer in beat wave process will be maximal. This maximally developed space-charge mode along with density ripple gives rise to strong nonlinear current responsible for the maximum THz amplitude. The amplitude of THz wave decreases as one moves away from the resonance position. At the same time α has maximum value (or λ_c is small) at resonance $\omega \sim \omega_h$; thus, density ripples with small corrugation factor (λ_c) are best suited for efficient THz excitation. This result matches with the observation of Antonsen *et al.* (2007), who proposed that the phase-matching requirements for efficient energy transfer from laser pulse to THz can be matched in a parabolic plasma channel (in radius) by z sequence of δ-function peaks with period d and strength triangle Δ, in axial distance, that is, $n_0(r, z) = n_{00}[1 + r^2/2r_{ch}^2 + \Delta \sum_{l=-\infty}^{\infty} \delta(z - ld)$.

Here, δ function-type axial coagulated plasma density acts as ripples. This inhomogeneity couples with the density perturbation provided by ponderomotive force and gives rise to a nonlinear current responsible for THz generation. Figure 3a shows that the THz amplitude increases with b for $b < 1.5$. The maximum amplitude (E_y) is obtained for Gaussian laser profile ($b = 0$) at resonance condition $\omega \approx \omega_h$. For higher value of decenterd parameter ($1.5 \le b \le 5$), the normalized THz amplitude increases with b and the maximum amplitude is again achieved at THz frequency $\omega \sim \omega_h$ as shown in Figure 3b. THz amplitude (E_y) achieves maximum value for hollow-Gaussian beating lasers (with $b = 5$). The variation of THz amplitude with b can be attributed to the variation of nonlinear ponderomotive force, which depends upon the shape of beating lasers beams as shown in Figure 2. Figure 3 also exhibits that the normalized THz field amplitude decreases and peak shifts toward higher value of THz due to new resonance frequency $\sqrt{\omega_p^2 + \omega_c^2}$ by varying applied magnetic field from $B_0 = 71$ kG ($\omega_c/\omega_p = 0.2$) to $B_0 = 107$ kG ($\omega_c/\omega_p = 0.3$). Thus, THz amplitude (at a particular THz frequency) can be tuned by changing dc magnetic field.

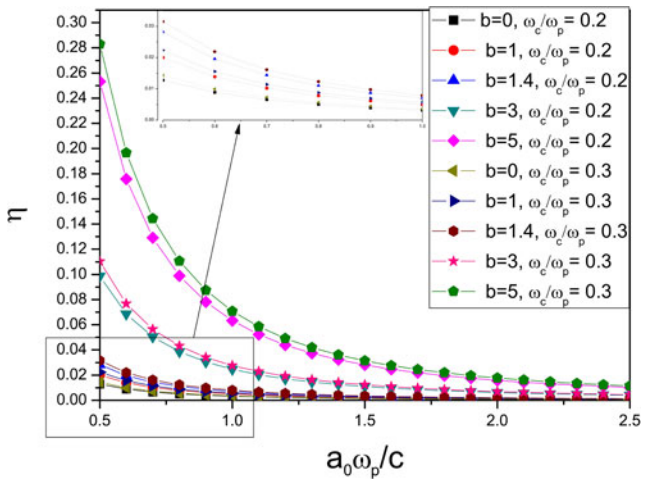

Fig. 4. Plot of THz efficiency (η) as a function of normalized laser beam width $a_o\omega_p/c$ for different values of b and ω_c/ω_p. Other normalized parameters are same as in Figure 1.

Finally, we calculate the efficiency (η) of the present scheme. Average EM energy stored per unit volume in electric and magnetic fields are given by the relations (Malik *et al.*, 2011, 2012*b*; Singh *et al.*, 2013; Varshney *et al.*, 2013, 2015) $\langle W_{Ei}\rangle = \frac{1}{8\pi}\varepsilon_0 \frac{\partial}{\partial\omega_i}\left[\omega_i\left(1 - \omega_p^2/\omega_i^2\right)\right]\langle|E_i|^2\rangle$ and $\langle W_{Bi}\rangle = \langle|B_i^2|\rangle/8\pi\mu_0$, respectively; where $\langle B_i\rangle = k\langle E_i\rangle/\omega_i$. The energy densities of the incident lasers (W_{pump}) and emitted radiation (W_{THz}) are as follows:

$$W_{pump} = \frac{\varepsilon_0 a_0}{2}|E_0|^2\sqrt{\frac{\pi}{2}}\left\{1 + \exp\left[\frac{b^2}{2}\right]\right\} \tag{12}$$

and

$$W_{THz} = \varepsilon_0|E_0|^2\left[\begin{array}{l}\frac{1}{2}\sqrt{\frac{\pi}{2}}(\xi_1^2\delta_{11}^2 + \xi_2^2\delta_{21}^2)a_0\{1 + e^{b^2/2}\} \\ +\frac{1}{2}\sqrt{\frac{\pi}{2}}(\xi_1^2\delta_{12}^2 + 4\xi_2^2\delta_{22}^2)a_0\{1 + (1 + b^2)e^{b^2/2}\} \\ -\frac{b^2}{a_0}\sqrt{\frac{\pi}{2}}(\xi_1^2\delta_{12}^2 + \xi_2^2\delta_{22}^2)\{-1 + e^{b^2/2}\}\end{array}\right]. \tag{13}$$

The normalized efficiency of THz radiation generation is evaluated

$$\eta = \frac{W_{THz}}{W_{pump}} = \left[(\xi_1'^2\delta_{11}'^2 + \xi_2'^2\delta_{21}'^2) + \frac{1}{a_0'^2}(\xi_1'^2\delta_{12}'^2 + 4\xi_2'^2\delta_{22}'^2).\right.$$
$$\left.\frac{\{1 + (1 + b^2)e^{b^2/2}\}}{\{1 + e^{b^2/2}\}} + \frac{b^2}{a_0'}(\xi_1'^2\delta_{12}'^2 + \xi_2'^2\delta_{22}'^2)\frac{\{1 - e^{b^2/2}\}}{\{1 + e^{b^2/2}\}}\right]. \tag{14}$$

Figure 4 shows that the efficiency η of the present scheme increases with decentered parameter (b) and decrease with laser beam width (a_0). The efficiency can be optimized with an applied static magnetic field corresponding to THz frequency. An efficiency ∼20% is achieved by frequency mixing of two hollow-Gaussian laser beams at beam width $a_0 \sim 3c/5\omega_p$ and dc magnetic field $B_0 \sim 107$ kG. Wu *et al.* (2008) achieved energy conversion efficiency ∼0.005 in inhomogeneous plasma at peak laser intensity 5.48×10^{12} W/cm^2, which is much lower than the present model. Malik *et al.* (2011, 2012*b*) have reported the conversion efficiency

https://doi.org/10.1017/S0263034617000167 Published online by Cambridge University Press

~0.002 and ~0.006 by beating of two spatial-Gaussian lasers and two super Gaussian lasers, respectively. Varshney *et al.* (2013) have reported the conversion efficiency $\sim 10^{-3}$ by beating of two planer *x*-mode lasers in a magnetized plasma. Further Varshney *et al.* (2015) improved one order of conversion efficiency and achieved $\sim 10^{-2}$ by photomixing of two super-Gaussian laser. Malik *et al.* (2014) obtain efficiency about 15% by frequency mixing of two top-hat lasers in the magnetized plasma.

4. CONCLUSIONS

The resonant excitation of THz radiation by beating of two cosh-Gaussian laser beams in preformed corrugated plasma in the presence of magnetic field is found to be quite efficient technique for obtaining intense, focused, and tunable THz beam. Nonlinear photomixing of laser beams result into a strong nonlinear ponderomotive force on plasma electrons, which in turn resonantly excites a nonlinear current responsible for THz radiation generation. The ponderomotive force depends upon the laser profile (which depends upon the decentralized parameter of cosh-Gaussian laser beams). Ponderomotive force decreases from $b = 0$ (Gaussian) to $b = 1.4$ (flat-top), and then starts increasing and maximizes for $b = 5$ (hollow-Gaussian). As a result, nonlinear current generated by using hollow-Gaussian laser beams exhibit the maximum THz field amplitude. THz field amplitude is optimized utilizing externally applied dc magnetic field. Here magnetic field plays two roles. It controls the phase velocity and group velocity of beating lasers on one side and the polarization of generated THz wave on the other. THz field amplitude acquires large values as ω approaches toward resonance frequency ($\sim\omega_h$). Stronger magnetic field leads to THz amplitude with the enhanced efficiency of the process, and intense radiation have been achieved when the lasers of lower beam width are used under the effect of stronger magnetic field and larger amplitude of the density ripples. In the presence of a stronger magnetic field, the ripples in the density are required to be created at comparatively smaller distances. Thus, the presence of transverse magnetic field makes the present scheme more tunable in terms of THz frequency. The efficiency can be further enhanced by using large amplitude density ripples.

ACKNOWLEDGEMENTS

One of the authors, P. V. acknowledges SERB-DST, Government of India for providing financial support.

REFERENCES

Abo-Bakr, M., Feikes, J., Holldack, K., Kuske, P., Peatman, W.B., Schade, U., Wustefeld, G. & Hübers, H.W. (2003). Brilliant, coherent far-infrared (THz) synchrotron radiation. *Phys. Rev. Lett*. **90**, 094801.

Antonsen, T.M., Palastra, J.J. & Milchberg, H.M. (2007). Excitation of terahertz radiation by laser pulses in nonuniform plasma channels. *Phys. Plasmas* **14**, 033107.

Bhasin, L. & Tripathi, V.K. (2011). Terahertz generation from laser filaments in the presence of a static electric field in a plasma. *Phys. Plasma* **18**, 123106.

Carr, G.L., Martin, M.C., McKinney, W.R., Jordan, K., Neil, G.R. & Williams, G.P. (2002). High-power terahertz radiation from relativistic electrons. *Nature (Lond.)* **420**, 153.

Dragoman, D. & Dragoman, M. (2004). Terahertz fields and applications. *Progr. Quantum Electron*. **28**, 1.

Hamster, H., Sullivan, A., Gordon, S. & Falcone, R.W. (1994). Short-pulse terahertz radiation from high-intensity-laser-produced plasmas. *Phys. Rev. E* **49**, 671.

Hamster, H., Sullivan, A., Gordon, S., White, W. & Falcone, R.W. (1993). Subpicosecond, electromagnetic pulses from intense laser-plasma interaction. *Phys. Rev. Lett*. **71**, 2725.

Hazra, S., Chini, T.K., Sanyal, M.K., Grenzer, J. & Pietsch, U. (2004). Ripple structure of crystalline layers in ion-beam-induced Si wafers. *Phys. Rev. B* **70**, 121307.

Kuo, C.-C., Pai, C.-H., Lin, M.-W., Lee, K.-H., Lin, J.-Y., Wang, J. & Chen, S.-Y. (2007). Enhancement of relativistic harmonic generation by an optically preformed periodic plasma waveguide. *Phys. Rev. Lett*. **98**, 033901.

Leemans, W.P., Tilborg, J.V., Faure, J., Geddes, C.G.R., Toth, C., Schroeder, C.B., Esarey, E., Fubioni, G. & Dugan, G. (2004). Terahertz radiation from laser accelerated electron bunches. *Phys. Plasmas* **11**, 2899.

Liu, C.S. & Tripathi, V.K. (2009). Tunable terahertz radiation from a tunnel ionized magnetized plasma cylinder. *J. Appl. Phys*. **105**, 013313.

Malik, A.K., Malik, H.K. & Nishida, Y. (2011). Terahertz radiation generation by beating of two spatial-Gaussian lasers. *Phys. Lett. A* **375**, 1191.

Malik, A.K., Malik, H.K. & Stroth, U. (2012*b*). Terahertz radiation generation by beating of two spatial-Gaussian lasers in the presence of a static magnetic field. *Phys. Rev. E* **85**, 016401.

Malik, A.K., Singh, K.P. & Sajal, V. (2014). Highly focused and efficient terahertz radiation generation by photo-mixing of lasers in plasma in the presence of magnetic field. *Phys. Plasmas* **21**, 065736.

Malik, H.K. (2015). Terahertz radiation generation by lasers with remarkable efficiency in electron positron plasma. *Phys. Lett. A* **379**, 2826–2829.

Malik, H.K. & Malik, A.K. (2011). Tunable and collimated terahertz radiation generation by femtosecond laser pulses. *Appl. Phys. Lett*. **99**, 251101.

Malik, H.K. & Malik, A.K. (2012). Strong and collimated terahertz radiation by super-Gaussian lasers. *Europhys. Lett*. **100**, 45001.

Malik, H.K. & Malik, A.K. (2013). Tuning and focusing of Terahertz radiation by dc magnetic field in a laser beating process. *IEEE J. Quantum Electron*. **49**, 232.

Penano, J., Sprangle, P., Hafizi, B., Gordon, D. & Serafim, P. (2010). Terahertz generation in plasmas using two-color laser pulses. *Phys. Rev. E* **81**, 026407.

Schillinger, H. & Sauerbrey, R. (1999). Electrical conductivity of long plasma channels in air generated by self-guided femtosecond laser pulses. *Appl. Phys. B: Lasers Opt*. **68**, 753.

Schroeder, C.B., Esarey, E., Tilborg, J.V. & Leemans, W.P. (2004). Theory of coherent transition radiation generated at a plasma-vacuum interface. *Phys. Rev. E* **69**, 016501.

Siegel, P.H. (2004). Terahertz technology in biology and medicine, Microwave Symposium Digest, IEEE MTT-S Int., 1575.

Singh, D. & Malik, H.K. (2014). Terahertz generation by mixing of two super Gaussian laser beams in collisional plasma. *Phys. Plasma* **21**, 083105.

Singh, D. & Malik, H.K. (2015). Enhancement of terahertz emission in magnetized collisional plasma. *Plasma Sources Sci. Technol*. **24**, 045001.

Singh, D. & Malik, H.K. (2016). Emission of strong terahertz pulses from laser wakefields in weakly coupled plasma. *Nucl. Instrum. Method Phys. Res. A* **829**, 403–407.

Singh, M., Singh, R.K. & Sharma, R. (2013). THz generation by cosh-Gaussian lasers in a rippled density plasma. *Europhys. Lett*. **104**, 35002.

Sizov, F. (2010). THz radiation sensors. *Opto-Electron. Rev*. **18**, 10.

Sprangle, P., Penano, J., Hafizi, B. & Kapetanakos, C. (2004). Ultrashort laser pulses and electromagnetic pulse generation in air and on dielectric surfaces. *Phys. Review E*. **69**, 066415.

Tripathi, D., Bhasin, L., Uma, R. & Tripathi, V. (2010). Terahertz generation by an amplitude-modulated Gaussian laser beam in a rippled density plasma column. *Phys. Scr*. **82**, 035504.

Varshney, P., Sajal, V., Chauhan, P., Kumar, R. & Sharma, N.K. (2014). Effects of transverse static electric field on terahertz radiation generation by beating of two transversely modulated Gaussian laser beams in a plasma. *Laser Part. Beams* **32**, 375.

Varshney, P., Sajal, V., Singh, K.P., Kumar, R. & Sharma, N.K. (2013). Strong terahertz radiation generation by beating of extra-ordinary mode lasers in a rippled density magnetized plasma. *Laser Part. Beams* **31**, 337.

Varshney, P., Sajal, V., Sharma, N.K., Chauhan, P. & Kumar, R. (2015). Strong terahertz radiation generation by beating of two x-mode spatial triangular lasers in a magnetized plasma. *Laser Part. Beams* **33**, 51.

Wu, H.C., Sheng, Z.M. & Zhang, J. (2008). Single-cycle powerful megawatt to gigawatt terahertz pulse radiated from a wavelength-scale plasma oscillator. *Phys. Rev. E* **77**, 046405.

Yoshii, J., Lai, C., Katsouleas, T., Joshi, C. & Mori, W. (1997). Radiation from Cerenkov wakes in a magnetized plasma. *Phys. Rev. Lett*. **79**, 4194.

https://doi.org/10.1017/S0263034617000167 Published online by Cambridge University Press